Synthesis, Characterization, and Electrochemical Properties of Organotransition Metal Fullerene Derivatives Containing dppf Ligands. Crystal Structures of *fac*-Mo(CO)$_3$(dppf)(CH$_3$CN), W(CO)$_4$(dppf), and *mer*-W(CO)$_3$(dppf)(η^2-C$_{60}$)

Li-Cheng Song,*,† Jin-Ting Liu,† Qing-Mei Hu,† Guan-Feng Wang,† Piero Zanello,‡ and Marco Fontani‡

Department of Chemistry, State Key Laboratory of Elemento-Organic Chemistry, Nankai University, Tianjin 300071, China, and Dipartimento di Chimica dell'Università di Siena, Via Aldo Moro, I-53100 Siena, Italy

Received July 5, 2000

Reaction of Mo(CO)$_3$(CH$_3$CN)$_3$ with an equimolar amount of 1,1′-bis(diphenylphosphino)-ferrocene (dppf) in refluxing acetonitrile gives rise to *fac*-Mo(CO)$_3$(dppf)(CH$_3$CN) (**1**) in 51% yield. While **1** reacts with [60]fullerene in chlorobenzene at about 90 °C to produce an isomeric mixture of *fac*/*mer*-Mo(CO)$_3$ (dppf)(η^2-C$_{60}$) (**2**) in 21% yield, the photolysis of Mo(CO)$_4$(dppf) and [60]fullerene in chlorobenzene at ambient temperature affords **2** in 87% yield. Similarly, *mer*-W(CO)$_3$(dppf)(η^2-C$_{60}$) (**3**), [*mer*-W(CO)$_3$(dppf)]$_2$(η^2,η^2-C$_{60}$) (**4**), *mer*-W(CO)$_3$(dppf) (η^2-C$_{70}$) (**5**), and [*mer*-W(CO)$_3$ (dppf)]$_2$(η^2,η^2-C$_{70}$) (**6**) can be prepared by photolysis of W(CO)$_4$(dppf) with [60]- or [70]fullerene in 87%, 13%, 51%, and 48% yields, respectively. While all the new compounds **1**−**6** have been characterized by elemental analyses and spectroscopic techniques, the structures of **1**, W(CO)$_4$(dppf), and **3** have been confirmed by single-crystal X-ray diffraction analyses. The cyclic voltammetric responses of **2** and **3** show that their sequential fullerene-centered reductions are shifted toward more negative potential values by about 0.2 V with respect to those of free C$_{60}$. Such a negative shift is quite similar to that previously observed for the related complexes W(CO)$_3$(dppb)(η^2-C$_{60}$) and Mo(CO)$_3$(dppe)(η^2-C$_{60}$). Moreover, the fullerene-centered reductions of **5** are negatively shifted by about 0.1 V with respect to free C$_{70}$, thus supporting that the η^2-coordination of the W(CO)$_3$(dppf) fragment to fullerenes causes a higher electronic interaction with C$_{60}$ than with C$_{70}$.

Introduction

Since the first preparation of organotransition metal fullerene complexes,[1] the organometallic chemistry of [60]- and [70]fullerenes has been receiving great attention.[2] Conceivably [60]- and [70]fullerenes can form organometallic complexes with single, double, triple, or multiple metal centers in a variety of coordination modes from η^1 to η^6. In fact, some of these types of transition metal fullerene complexes have been already prepared and structurally characterized.[3−6] We are interested in the synthesis, characterization, and properties of organotransition metal fullerene derivatives.[7] As a continuation of our project related to the chemistry of transition metal fullerene complexes, we recently initiated studies on the thermal reaction of *fac*-Mo(CO)$_3$(dppf)(CH$_3$CN) with C$_{60}$ and photolysis of Mo(CO)$_4$(dppf) with C$_{60}$ and W(CO)$_4$(dppf) with C$_{60}$ or C$_{70}$ to see if the corresponding heteronuclear transition metal M/Fe (M = Mo, W) fullerene complexes could be prepared. Fortunately, we have obtained such expected complexes from these reactions, namely, *fac*/*mer*-Mo(CO)$_3$(dppf)(η^2-C$_{60}$), *mer*-W(CO)$_3$(dppf)(η^2-C$_{60}$), [*mer*-W(CO)$_3$(dppf)]$_2$(η^2,η^2-C$_{60}$), *mer*-W(CO)$_3$(dppf)(η^2-C$_{70}$), and [*mer*-W(CO)$_3$ (dppf)]$_2$(η^2,η^2-C$_{70}$). It is worth noting that such heteronuclear transition metal C$_{60}$ derivatives are rare,[6e] and up to now no C$_{70}$ heteronuclear transition metal derivatives, to our knowledge, have appeared in the literature. Herein we report the synthesis, spectroscopic characterization, and electrochemistry of these new C$_{60}$ and C$_{70}$ heteronuclear transition metal derivatives, as well as the crystal structures of two starting materials and one of the fullerene derivatives.

Results and Discussion

Synthesis, Spectroscopic Characterization, and Crystal Structure of *fac*-Mo(CO)$_3$ (dppf)(CH$_3$CN) (1). Treatment of Mo(CO)$_3$(CH$_3$CN)$_3$ with an equimolar quantity of 1,1′-bis(diphenylphosphino)ferrocene (dppf) in boiling acetonitrile for 30 h resulted in formation of **1** in 51% yield, as shown in eq 1.

Compound **1** is an air-sensitive, golden solid, which might exist as another isomeric form, namely, the *mer*

* To whom correspondence should be addressed. Fax: 0086-22-23504853. E-mail: lcsong@public.tpt.tj.cn.
† Nankai University.
‡ Università di Siena.

(1) Fagan, P. J.; Calabrese, J. C.; Malone, B. *Science* **1991**, *252*, 1160.
(2) For reviews, see for example: (a) Fagan, P. J.; Calabrese, J. C.; Malone, B. *Acc. Chem. Res.* **1992**, *25*, 134. (b) Green, M. L. H. *Pure Appl. Chem.* **1995**, *67*, 249. (c) Sliwa, W. *Transition Met. Chem.* **1996**, *21*, 583. (d) Balch, A. L.; Olmstead, M. M. *Chem. Rev.* **1998**, *98*, 2123. (e) Sokolov, V. I. *Pure Appl. Chem.* **1998**, *70*, 789.

10.1021/om000579+ CCC: $19.00
Publication on Web 11/10/2000

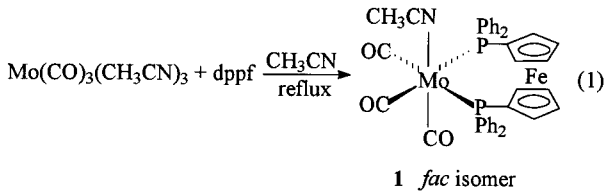

1 *fac* isomer

isomer. However, the X-ray diffraction analysis has shown that it is actually the *fac* isomer. The molecular ORTEP diagram of **1** is shown in Figure 1, whereas Table 1 lists its selected bond lengths and angles. As seen in Figure 1, compound **1** contains one CH_3CN ligand bonded to Mo via its N atom and *cis* to both of the phosphorus atoms P(1) and P(2) of the dppf ligand. That is, **1** adopts the *fac* configuration. The dppf ligand is chelated to the Mo atom with a bite angle of 97.800(19)°. This bite angle is very close to corresponding bite angles of *fac*-$W(CO)_3(dppf)(CH_3CN)$ (98.05(6)°)[8] and $Mo(CO)_4(dppf)$ (95.28(2)°).[9] The two cyclopentadienyl rings in the dppf ligand are almost parallel with a dihedral angle of 2.37(0.09)° and staggered to each other. While the IR spectrum of **1** shows three absorption bands in the region 1808−1926 cm^{-1} for its terminal carbonyls,[10] the ^1H NMR spectrum of **1** exhibits a multiplet around 7.40 ppm assigned to its phenyl groups and a singlet at 1.98 ppm to its methyl group. In addition, the ^{31}P NMR spectrum of **1** displays only one singlet at 37.86 ppm, which is consistent with its *fac* configuration, cofirmed by single-crystal X-ray diffraction analysis. This is because the *fac* isomer has two magnetically identical P atoms, whereas the *mer* isomer has two magnetically different P atoms.[11]

Synthesis and Spectroscopic Characterization of *fac/mer*-$Mo(CO)_3(dppf)(\eta^2\text{-}C_{60})$ (2). When an equimolar quantity of **1** was added to a solution of C_{60} in chlorobenzene followed by stirring and heating the mixture at about 90 °C for 2 h, a dark green solution was formed. Further treatment of this resulting solution by column chromatography afforded **2** in 21% yield. However, when an equimolar mixture of $Mo(CO)_4(dppf)$ and C_{60} in chlorobenzene was irradiated with a UV 450 W photochemical lamp at room temperature for 2 h, compound **2** was obtained in a much higher yield (87%), as shown in eq 2.

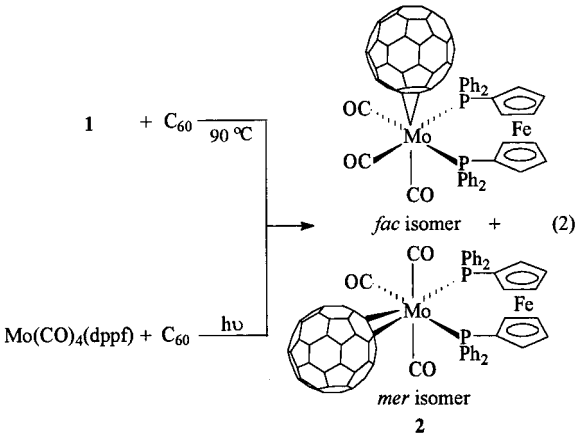

Compound **2** is an air-sensitive, dark green solid, which slightly dissolves in polar solvents such as chloroform, toluene, THF, carbon disulfide, and chlorobenzene, but does not dissolve in nonpolar solvents such as hexane and petroleum ethers. Obviously, this C_{60} derivative, just like its precursor **1**, might exist as a *fac* isomer, a *mer* isomer, or as a mixture of the *fac* and *mer* isomers. In fact, the ^{31}P NMR spectrum of **2** indicated that it exists as an isomeric mixture of the *fac* and *mer* isomers. This is because that the ^{31}P NMR spectrum of **2** (Figure 2) shows two doublets at 39.31 and 29.86 ppm assignable to the two different P atoms in the *mer* isomer and a singlet at 33.56 ppm assignable to the two identical P atoms of the *fac* isomer. The IR spectrum of **2** displays four bands in the range 1434−526 cm^{-1} for its C_{60} core[12] and five bands in the region 2000−1882 cm^{-1} for its terminal carbonyls.[10] The latter is in good agreement with **2** being a mixture of the two isomers, since the number of IR active bands cannot exceed but may be less than the number of CO ligands in the complex.[13]

(3) For mononuclear fullerene derivatives, see: (a) Balch, A. L.; Catalano, V. J.; Lee, J. W. *Inorg. Chem.* **1991**, *30*, 3980. (b) Balch, A. L.; Catalano, V. J.; Lee, J. W.; Olmstead, M. M.; Parkin, S. R. *J. Am. Chem. Soc.* **1991**, *113*, 8953. (c) Balch, A. L.; Catalano, V. J.; Lee, J. W.; Olmstead, M. M. *J. Am. Chem. Soc.* **1992**, *114*, 5455. (d) Ballenweg, S.; Gleiter, R.; Krätschmer, W. *Tetrahedron Lett.* **1993**, *34*, 3737. (e) Bashilov, V. V.; Petrovskii, P. V.; Sokolov, V. I.; Lindeman, S. V.; Guzey, I. A.; Struchkov, Y. T. *Organometallics* **1993**, *12*, 991. (f) Sawamura, M.; Iikura, H.; Nakamura, E. *J. Am. Chem. Soc.* **1996**, *118*, 12850. (g) Tang, K.; Zheng, S.; Jin, X.; Gu, Z.; Zhou, X.; Tang, Y. *J. Chem. Soc., Dalton Trans.* **1997**, 3585. (h) Wijnkoop, M. V.; Meidine, M. F.; Avent, A. G.; Darwish, A. D.; Kroto, H. W.; Taylor, R.; Walton, D. R. M. *J. Chem. Soc., Dalton Trans.* **1997**, 675. (i) Chernega, A. N.; Green, M. L. H.; Haggitt, J.; Stephens, A. H. H. *J. Chem. Soc., Dalton Trans.* **1998**, 755. (j) Maruyama, H.; Fujiwara, M.; Tanaka, K. *Chem. Lett.* **1998**, 805. (k) Hsu, H.-F.; Du, Y.; Albrecht-Schmitt, T. E.; Wilson, S. R.; Shapley, J. R. *Organometallics* **1998**, *17*, 1756. (l) Bengough, M. N.; Thompson, D. M.; Baird, M. C. *Organometallics* **1999**, *18*, 2950. (m) Burlakov, V. V.; Usatov, A. V.; Lyssenko, K. A.; Antpin, M. Yu.; Novikov, Yu. N.; Shur, V. B. Eur. *J. Inorg. Chem.* **1999**, 1855.

(4) For dinuclear fullerene derivatives, see: (a) Balch, A. L.; Lee, J. W.; Noll, B. C.; Olmstead, M. M. *J. Am. Chem. Soc.* **1992**, *114*, 10984. (b) Balch, A. L.; Lee, J. W.; Olmstead, M. M. *Angew. Chem., Int. Ed. Engl.* **1992**, *31*, 1356. (c) Zhang, S.; Brown, T. L.; Du, Y.; Shapley, J. R. *J. Am. Chem. Soc.* **1993**, *115*, 6705. (d) Balch, A. L.; Lee, J. W.; Noll, B. C.; Olmstead, M. M. *Inorg. Chem.* **1994**, *33*, 5238. (e) Mavunkal, I. J.; Chi, Y.; Peng, S.-M.; Lee, G.-H. *Organometallics* **1995**, *14*, 4454.

(5) For trinuclear fullerene derivatives, see: (a) Hsu, H.-F.; Shapley, J. R. *J. Am. Chem. Soc.* **1996**, *118*, 9192. (b) Hsu, H.-F.; Shapley, J. R. *J. Chem. Soc., Chem. Coommun.* **1997**, 1125. (c) Park, J. T.; Song, H.; Cho, J.-J.; Chung, M.-K.; Lee, J.-H.; Suh, I.-H. *Organometallics* **1998**, *17*, 227. (d) Song, H.; Lee, K.; Park, J. T.; Choi, M.-G. *Organometallics* **1998**, *17*, 4477.

(6) For multinuclear fullerene derivatives, see: (a) Fagan, P. J.; Calabrese, J. C.; Malone, B. *J. Am. Chem. Soc.* **1991**, *113*, 9408. (b) Rasinkangas, M.; Pakkaned, T. T.; Pakkaned, T. A.; Ahlgrén, M.; Rouvinen, J. *J. Am. Chem. Soc.* **1993**, *115*, 4901. (c) Balch, A. L.; Hao, L.; Olmstead, M. M. *Angew. Chem., Int. Ed. Engl.* **1996**, *35*, 188. (d) Lee, K.; Hsu, H.-F.; Shapley, J. R. *Organometallics* **1997**, *16*, 3876. (e) Lee, K.; Shapley, J. R. *Organometallics* **1998**, *17*, 3020.

(7) (a) Song, L.-C.; Zhu, Y.-H.; Hu, Q.-M. *Polyhedron* **1997**, *16*, 2141. (b) Song, L.-C.; Zhu, Y.-H.; Hu, Q.-M. *Polyhedron* **1998**, *17*, 469. (c) Song, Y.-L.; Fang, G.-Y.; Wang, Y.-X.; Liu, C.-F.; Song, L.-C.; Zhu, Y.-H.; Hu, Q.-M. *Appl. Phys. Lett.* **1999**, *74*, 1. (d) Song, L.-C.; Zhu, Y.-H.; Hu, Q.-M. *J. Chem. Res., Synop.* **1999**, 56. (e) Song, L.-C.; Liu, J.-T.; Hu, Q.-M.; Weng, L.-H. *Organometallics* **2000**, *19*, 1643.

(8) Hsu, S. C. N.; Yeh, W.-Y.; Chiang, M. Y. *J. Organomet. Chem.* **1995**, *492*, 121.

(9) Butler, I. R.; Cullen, W. R.; Kim, T.-J.; Rettig, S. J.; Trotter, J. *Organometallics* **1985**, *4*, 972.

(10) Darenbourg, D. J.; Zalewski, D. J.; Plepys, C.; Campana, C. *Inorg. Chem.* **1987**, *26*, 3727.

(11) (a) Issacs, E. E.; Graham, W. A. G. *Inorg. Chem.* **1975**, *14*, 2560. (b) Bond, A. M.; Colton, R.; McGregor, K. *Inorg. Chem.* **1986**, *25*, 2378.

(12) Hare, J. P.; Dennis, T. J.; Kroto, H. W. Taylor, R.; Allaf, A. W.; Balm, S.; Walton, D. R. M. *J. Chem. Soc., Chem. Commun.* **1991**, 412.

(13) Collman, J. P.; Hegedus, L. S.; Norton, J. R.; Finke, R. J. *Principles and Applications of Organotransition Metal Chemistry*, 2nd ed.; University Science Books: Mill Valley, CA, 1987.

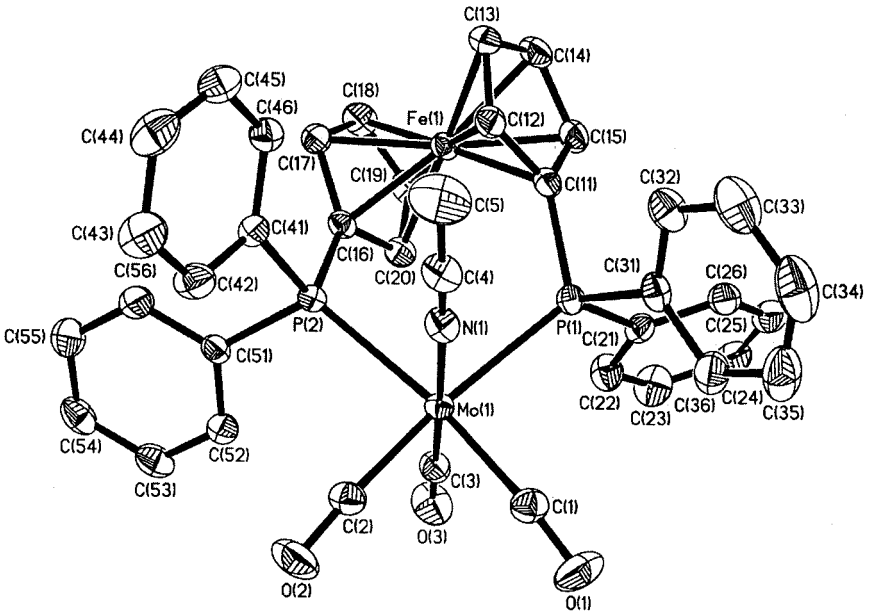

Figure 1. ORTEP diagram of **1** with ellipsoids drawn at 30% probability.

Table 1. Selected Bond Lengths (Å) and Angles (deg) for 1

Mo(1)−C(3)	1.946(3)	Mo(1)−P(1)	2.5985(6)
Mo(1)−C(2)	1.962(3)	Fe(1)−C(16)	2.026(2)
Mo(1)−C(1)	1.967(3)	Fe(1)−C(18)	2.067(2)
Mo(1)−N(1)	2.222(2)	P(1)−C(11)	1.821(2)
Mo(1)−P(2)	2.5702(6)	P(2)−C(16)	1.812(2)
C(3)−Mo(1)−C(2)	87.18(10)	C(1)−Mo(1)−P(2)	173.22(8)
C(3)−Mo(1)−C(1)	83.94(10)	N(1)−Mo(1)−P(2)	85.53(5)
C(2)−Mo(1)−C(1)	84.63(11)	C(3)−Mo(1)−P(1)	97.92(7)
C(3)−Mo(1)−N(1)	177.67(9)	C(2)−Mo(1)−P(1)	170.84(8)
C(2)−Mo(1)−N(1)	93.67(9)	C(1)−Mo(1)−P(1)	88.33(8)
C(1)−Mo(1)−N(1)	98.30(9)	N(1)−Mo(1)−P(1)	81.53(5)
C(3)−Mo(1)−P(2)	92.31(7)	P(2)−Mo(1)−P(1)	97.800(19)
C(2)−Mo(1)−P(2)	89.56(8)		

In the UV−vis spectrum of **2**, those intense bands between 200 and 400 nm are close to those of free C_{60}. This is typical of a [60]fullerene cage which has been modified by complexation.[14] The biggest changes in the spectrum of **2** compared with that of free C_{60} appear in the visible range. A new band appearing at 436.3 nm might be the reason for the color change of the reaction mixture from purple C_{60} to dark green **2** and suggests that the [60]fullerene is coordinated to molybdenum in an η^2-fashion in the compound.[3i,7e,15] In addition, the ^{1}H NMR spectrum of **2** indicates the presence of corresponding phenyl and substituted cyclopentadienyl groups.

Synthesis and Spectroscopic Characterization of *mer*-W(CO)$_3$(dppf)(η^2-C$_{60}$) (3) and [*mer*-W(CO)$_3$(dppf)]$_2$(η^2,η^2-C$_{60}$) (4). Irradiation of an equimolar mixture of W(CO)$_4$(dppf) and C_{60} in chlorobenzene with a UV 450 W photochemical lamp at room temperature for 2 h gave rise to a dark green solution. Further treatment of this solution by TLC afforded **3** in 87% yield and **4** in 13% yield, as shown in eq 3.

Compounds **3** and **4** are air-stable solids, which are, similar to **2**, slightly soluble in those polar solvents, but not soluble in nonpolar solvents such as hexane and petroleum ethers. **3** and **4** have been characterized by elemental analysis, spectroscopic methods, and particularly for **3** X-ray diffraction. The ^{31}P NMR spectra indicated that they all have a meridional geometry, since the ^{31}P NMR spectrum of **3** shows two doublets at 18.47 and 12.79 ppm, and that of **4** exhibits two singlets at 23.67 and 16.94 ppm. This implies that they all contain two different P atoms and belong to the *mer* isomers. The IR spectra of **3** and **4** display four bands in the range 1434−514 cm^{-1} for their C_{60} cores[12] and three bands in the region 1998−1868 cm^{-1} for their terminal carbonyls.[10] The latter is in good agreement with the fact that **3** and **4** are single isomers, since the isomeric mixtures would have more IR active bands for

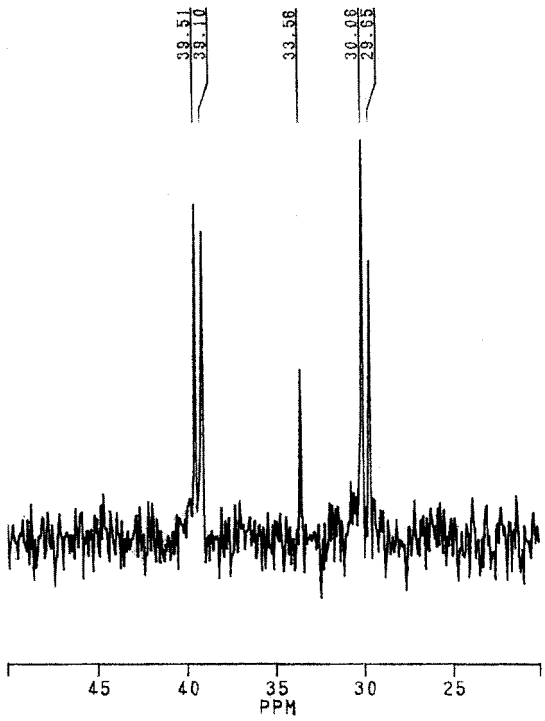

Figure 2. ^{31}P NMR spectrum of **2**.

(14) (a) Taylor, R.; Hare, J. P.; Abdul-Sada, A. K.; Kroto, H. W. *J. Chem. Soc., Chem. Commun.* **1990**, 1423. (b) Hare, J. P.; Kroto, H. W.; Taylor, R. *Chem. Phys. Lett.* **1991**, *177*, 394. (c) Akasaka, T.; Ando, W.; Kobagashi, K.; Nagase, S. *J. Am. Chem. Soc.* **1993**, *115*, 1605.

(15) Hirsch, A.; Grösser, T.; Skiebe, A.; Soi, A. *Chem. Ber.* **1993**, *126*, 1061.

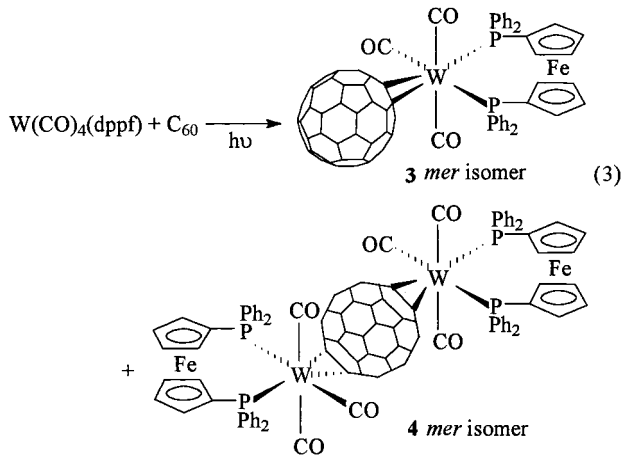

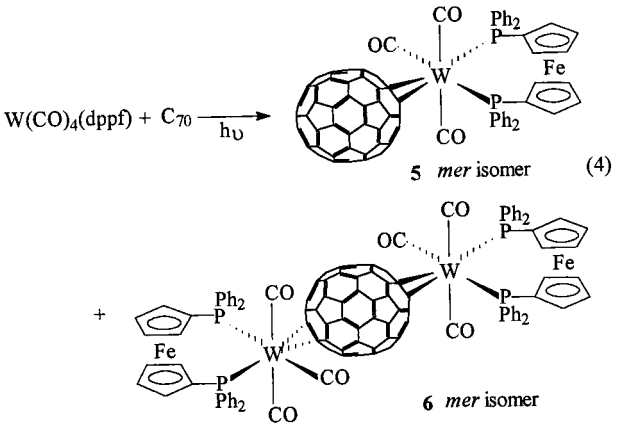

their terminal carbonyl ligands.[13] Similar to **2**, the UV−vis spectra of **3** and **4** also display three intense bands between 200 and 400 nm; the new bands appearing at 433.0 nm for **3** and at 430.5 nm for **4**, compared with free C_{60}, suggest that the C_{60} is coordinated to tungsten in an η^2-fashion in each of the compounds.[3i,7e,15]

A series of ^{13}C NMR studies of the C_{60} moiety for numerous metallofullerenes have been reported such as for $Rh(NO)(PPh_3)_2(\eta^2\text{-}C_{60})$ (C_s symmetry, showing 31 sp^2 and 1 sp^3 resonance signals)[16] and $Fe(CO)_4(\eta^2\text{-}C_{60})$ (C_{2v}, showing 16 sp^2 and 1 sp^3 resonance signals).[17] The chemical shifts of sp^2 and sp^3 carbon atoms of the C_{60} core are typically in the regions 175−135 ppm and 85−50 ppm, respectively. Although **3** possesses C_s symmetry, there are only 16 signals in the region 164−137 ppm and one signal at 79.34 ppm in its ^{13}C NMR spectrum for the carbon atoms of its C_{60} core. Among the 17 signals, one represents eight carbons, 10 could be each assigned to four carbon atoms, and the other six might be each assigned to two carbon atoms. This implies that the C_{60}-metal moiety rotation is present in the solution at room temperature, which renders the number of ^{13}C NMR signals of the C_{60} moiety varying from a 32-line pattern of C_s symmetry to a 17-line pattern of C_{2v} symmetry.[7e,16] It is fortunate that *mer* configuration of **3** has been confirmed by crystal X-ray diffraction analysis (see below). In theory, when the [60]-fullerene coordinates to two identical metal fragments in an η^2-fashion using its 6:6 bonds, the C_{60} metal complex may have eight possible regioisomers.[4d] However, the ^{31}P NMR spectrum of **4**, except showing evidence for its *mer* configuration as mentioned above, also suggests that the two identical metal fragments $W(CO)_3$(dppf) in **4** are bonded to 6:6 bonds at the opposite ends of the C_{60} portion. In fact, this sort of regioisomer was also observed for diiridium fullerene complexes.[4a,d]

Synthesis and Spectroscopic Characterization of *mer*-$W(CO)_3$(dppf)(η^2-C_{70}) (5) and [*mer*-$W(CO)_3$-(dppf)]$_2$(η^2,η^2-C_{70}) (6). Similarly, upon photolysis of an equimolar mixture of $W(CO)_4$(dppf) and C_{70} in chlorobenzene at room temperature for 2 h, a brown solution was formed. Further treatment of this solution by TLC afforded **5** in 51% yield and **6** in 48% yield, as shown in eq 4.

Compounds **5** and **6** are air-stable solids, which are, similar to **3** and **4**, slightly soluble in those polar solvents, but not soluble in the nonpolar solvents. These two [70]fullerene derivatives are single *mer* isomers, which have been characterized by elemental analysis, IR, ^1H NMR, ^{31}P NMR, and UV−vis spectroscopies. The ^{31}P NMR spectra of **5** and **6** each show two broader singlets centered at 16.65/10.20 ppm and at 12.27/5.54 ppm, each singlet being surrounded by satellite peaks due to coupling between P atoms and tungsten isotopes, such as isotope ^{183}W. This indicates that there are two different P atoms present in each of **5** and **6**; thus they are all *mer* isomers.

The IR spectra of **5** and **6** display several bands in the range 1636−535 cm^{-1} for their C_{70} cores[12] and three bands in the region 1999−1870 cm^{-1} for their terminal carbonyls.[10] This is also in good agreement with **5** and **6** being *mer* isomers**.** In the UV−vis spectra of **5** and **6** the intense bands between 200 and 400 nm are close to those of free C_{70}.[14] A new band appearing at ca. 457 nm instead of the band at 470 nm for free C_{70} might be attributed to the [70]fullerene being coordinated to the metal in an η^2-fashion.[3i,7e,15]

Since C_{70} has four nonequivalent reactive 6:6 bonds, its double addition would be very complicated. However, among the reactive 6:6 bonds of C_{70} the Ca−Cb bonds at the poles of the molecule have the highest degree of pyramidalization, thus are expected to be the most reactive.[4b] In fact, that C_{70} is bound to metals in an η^2-fashion with the Ca−Cb bonds has been confirmed by X-ray diffraction analysis for the known C_{70} metal complexes.[3b,k,4b] So, in the double addition product **6**, the C_{70} is most likely bonded to tungsten atoms through two Ca−Cb bonds at the poles of the C_{70} ligand. This coordination geometry for **6** is consistent with its IR and ^{31}P NMR spectra, since it displays only three bands for its terminal carbonyls and two groups of ^{31}P NMR signals. However, since there are three Ca−Cb bonds on the opposite poles, the exact structure of the double addition product **6** still remains to be solved in the future by X-ray diffraction analysis.

Crystal Structures of $W(CO)_4$(dppf) and 3. Fortunately, we succeeded in carrying out the X-ray diffraction analyses for starting material $W(CO)_4$(dppf) and its C_{60} derivative **3**. The molecular ORTEP diagrams of $W(CO)_4$(dppf) and **3** are shown in Figures 3 and 4,

(16) Green, M. L. H.; Stephens, A. H. H. *J. Chem. Soc., Chem. Commun.* **1997**, 793.

(17) Douthwaite, R. E.; Green, M. L. H.; Stephens, A. H. H.; Turner, J. F. C. *J. Chem. Soc., Chem. Commun.* **1993**, 1522.

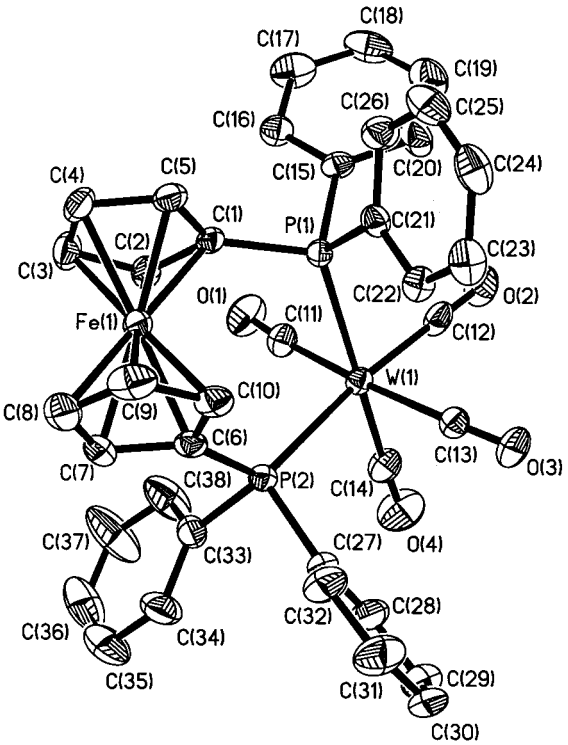

Figure 3. ORTEP diagram of $W(CO)_4$(dppf) with ellipsoids drawn at 30% probability.

Table 2. Selected Bond Lengths (Å) and Angles (deg) for $W(CO)_4$(dppf)

W(1)−C(14)	1.964(8)	W(1)−P(2)	2.5627(17)
W(1)−C(12)	1.982(7)	Fe(1)−C(1)	2.017(6)
W(1)−C(11)	2.021(7)	Fe(1)−C(4)	2.080(7)
W(1)−C(13)	2.029(7)	P(1)−C(1)	1.812(6)
W(1)−P(1)	2.5332(16)	P(2)−C(6)	1.833(7)
C(12)−W(1)−P(1)	89.3(2)	C(11)−W(1)−P(1)	84.5(2)
C(14)−W(1)−C(13)	87.4(3)	C(13)−W(1)−P(1)	98.99(19)
C(12)−W(1)−C(13)	88.1(3)	C(14)−W(1)−P(2)	89.7(2)
C(11)−W(1)−C(13)	172.2(3)	C(12)−W(1)−P(2)	174.3(2)
C(14)−W(1)−P(1)	172.1(2)	C(11)−W(1)−P(2)	98.8(2)
C(14)−W(1)−C(12)	86.1(3)	C(13)−W(1)−P(2)	87.87(18)
C(14)−W(1)−C(11)	88.6(3)	P(1)−W(1)−P(2)	95.24(5)
C(12)−W(1)−C(11)	85.0(3)		

whereas Tables 2 and 3 list their selected bond lengths and angles, respectively.

Figure 3 shows that $W(CO)_4$(dppf) contains a dppf ligand coordinated via its two P atoms to the W atom of the $W(CO)_4$ moiety, thus completing a *cis* octahedral coordination geometry for the W atom. However, the configuration at the metal center is distorted from a normal octahedral geometry, with the P(1)−W(1)−P(2) angle of 95.24(5)° increased from the ideal value of 90°, but comparable with those in *fac*-$W(CO)_3$(dppf)(CH_3CN) (98.05(6)°)[8] and $Mo(CO)_4$(dppf) (95.28(2)°).[9]

Figure 4 shows that **3** has a C_{60} ligand bound to the W atom of the $W(CO)_3$(dppf) unit in an η^2-fashion with the C(1)−C(2) bond between two six-membered rings, which results in a significant elongation of the fullerene C(1)−C(2) bond. The C(1)−C(2) bond length is 1.489(6) Å, which is considerably longer than the corresponding bond in free C_{60} (6:6 bond length 1.38 Å)[2d] and the average bond length (1.386 Å) of the other 29 6:6 bonds in **3**, due to the metal-to-C_{60} π-back-donation.[2a] Such bond lengthening is also observed in other η^2-C_{60} metal complexes, such as in $Pt(PPh_3)_2(\eta^2$-$C_{60})$ (1.50(3) Å),[1] Pd-

Table 3. Selected Bond Lengths (Å) and Angles (deg) for 3

W(1)−C(1)	2.316(4)	C(1)−C(9)	1.495(7)
W(1)−C(2)	2.338(4)	C(2)−C(12)	1.483(6)
W(1)−P(1)	2.5403(12)	C(2)−C(3)	1.482(6)
W(1)−P(2)	2.6375(13)	Fe(1)−C(69)	2.016(5)
W(1)−C(62)	2.008(6)	Fe(1)−C(71)	2.070(5)
W(1)−C(63)	2.014(6)	P(1)−C(64)	1.819(5)
W(1)−C(61)	2.036(6)	P(2)−C(69)	1.832(5)
C(1)−C(6)	1.471(6)	C(22)−C(23)	1.360(8)
C(1)−C(2)	1.489(6)	C(17)−C(18)	1.472(9)
C(1)−W(1)−P(2)	120.08(11)	C(1)−W(1)−C(2)	37.32(15)
P(1)−W(1)−P(2)	88.63(4)	C(62)−W(1)−P(1)	82.13(14)
C(62)−W(1)−C(63)	85.8(2)	C(63)−W(1)−P(1)	91.07(14)
C(62)−W(1)−C(61)	88.1(2)	C(61)−W(1)−P(1)	90.57(14)
C(63)−W(1)−C(61)	173.4(2)	C(1)−W(1)−P(1)	151.29(12)
C(62)−W(1)−C(1)	69.18(18)	C(2)−W(1)−P(1)	171.02(11)
C(63)−W(1)−C(1)	87.53(18)	C(62)−W(1)−P(2)	170.63(14)
C(61)−W(1)−C(1)	87.53(18)	C(63)−W(1)−P(2)	92.90(16)
C(62)−W(1)−C(2)	106.24(18)	C(61)−W(1)−P(2)	93.54(16)
C(63)−W(1)−C(2)	86.39(18)	C(2)−W(1)−P(2)	82.90(11)
C(61)−W(1)−C(2)	92.93(19)		

$(PPh_3)_2(\eta^2$-$C_{60})$ (1.45(3) Å),[3e] $W(CO)_3$(dppe)(η^2-C_{60}) (1.497(8) Å), $Mo(CO)_3$(dppe) (η^2-C_{60}) (1.483(10) Å),[3k] $Os_3(CO)_{11}$-(η^2-C_{60}) (1.42(3) Å),[5c] $RuCl(NO)(PPh_3)_2(\eta^2$-$C_{60})$ (1.489(7) Å),[3i] $Ir(CO)Cl(PPh_3)_2(\eta^2$-$C_{60})$ (1.53(3) Å),[3a] $Mo(CO)_3$-(dppb)(η^2-C_{60}) (1.477 (5) Å), $W(CO)_3$(dppb)(η^2-C_{60}) (1.501(11) Å),[7e] and $Cp_2Ti(\eta^2$-$C_{60})$ (1.510(2) Å).[3m]

The influence of such a coordination mode on the geometry of the C_{60} moiety is manifested not only in the lengthening of the C(1)−C(2) bond but also in the lengthening of the four bonds adjacent to C(1) and C(2) atoms. That is, as shown in Table 2, the C(1)−C(6), C(1)−C(9), C(2)−C(3), and C(2)−C(12) bond lengths are in the range 1.471(6)−1.495(7) Å (average 1.483 Å), whereas the average C−C distance at the other 5:6 ring junctions is 1.446 Å (1.45 Å in free fullerene).[2d] In addition, the two coordinated carbon atoms C(1) and C(2) are pulled away from the fullerene cage, as a result of which the C(1) and C(2) atoms deviate from the planes of the corresponding six-membered rings by ca. 0.16 and 0.18 Å, respectively. The distances from the centroid of the C_{60} ligand to the C(1) and C(2) atoms are 3.711 and 3.746 Å, whereas the corresponding distance to the other carbon atoms of C_{60} are in the range 3.501−3.548 Å.

The metal W atom has a slightly distorted octahedral geometry. The atoms W(1), C(1), C(2), C(62), P(1), and P(2) are coplanar (the plane equation gives a mean deviation of 0.0444 Å). A *mer* configuration around the W atom is adopted for the dppf and C_{60} ligands, where one phosphorus atom, P(1), of the chelating diphosphine is *trans* to C_{60} and the other, P(2), is *cis* to that center. Since the *trans* effect of the carbonyl ligand C(62)O(2) is stronger than that of the C_{60} ligand, the W(1)−P(2) bond length (2.6375(13) Å) is longer than that of W(1)−P(1) (2.5403(12) Å). The bite angle of the dppf ligand, P(1)−W(1)−P(2) (88.63(4)°), is smaller than those in $W(CO)_4$(dppf) (95.24(5)°), $W(CO)_3$(dppf)(CH_3CN) (98.05(6)°),[8] and $Mo(CO)_4$(dppf) (95.28(2)°),[9] but larger than that of the dppe ligand in $W(CO)_3$(dppe)(η^2-C_{60}) (79.0(1)°)[3k] or that of the dppb in $W(CO)_3$(dppb)(η^2-C_{60}) (77.04(8)°).[7e]

It is interesting to compare the dppf ligand of the C_{60} derivative **3** with that of its precursor $W(CO)_4$(dppf). As seen from Figures 3 and 4, the two dppf ligands are chelated to the W atom via P(1) and P(2) located on one

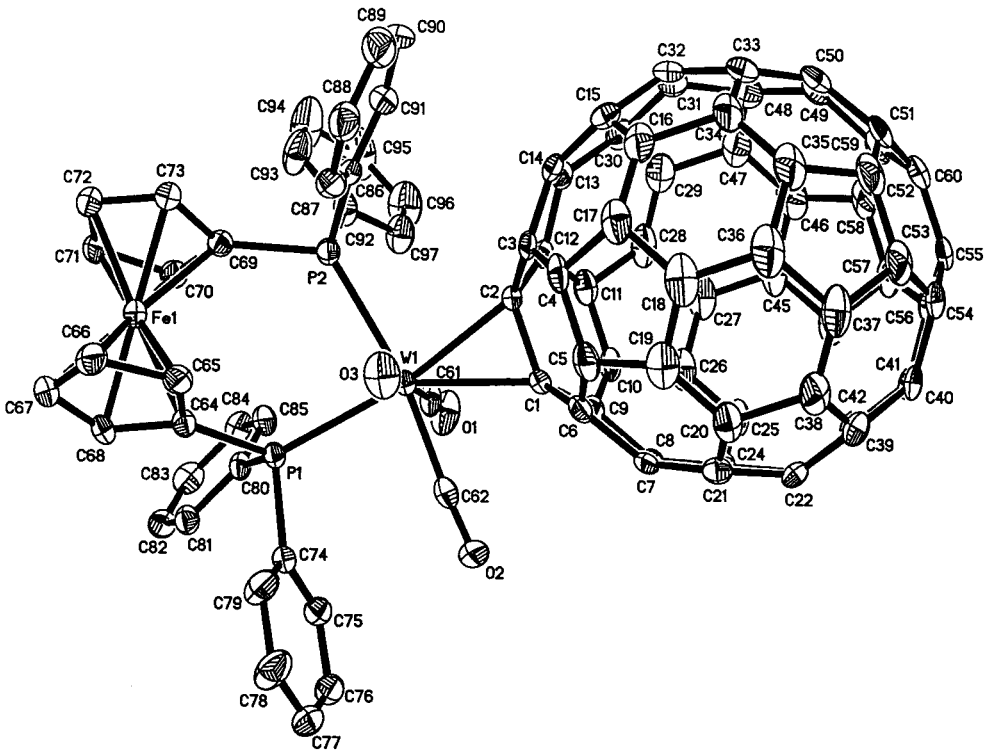

Figure 4. ORTEP diagram of **3** with ellipsoids drawn at 30% probability.

side of the ligands. The two cyclopentadienyl rings in dppf are planar within experimental error (the mean deviations are 0.0028 and 0.0052 Å for **3** and 0.0005 and 0.0077 Å for $W(CO)_4$(dppf)), whereas they deviate slightly from parallel with dihedral angles of 2.52(0.31)° and 3.73(0.35)° for $W(CO)_4$(dppf) and **3**, respectively. The C−C bond lengths in the cyclopentadienyl rings are all in the range 1.442(7)−1.400(8) Å. The P−C(Cp) bond lengths are 1.812(6) and 1.833(7) Å for $W(CO)_4$(dppf) and 1.829(5) and 1.832(5) Å for **3**. The Fe−C(Cp) bond lengths range from 2.017(6) to 2.080(7) Å for $W(CO)_4$-(dppf) and from 2.016(5) to 2.070(5) Å for **3**. The Fe−C(Cp) distances are shortest for the substituted C(1) (2.017(6) Å) and C(6) (2.041(6) Å) in $W(CO)_4$(dppf) and for C(69) (2.016(5) Å) and C(64) (2.023(5) Å) in **3**, which indicates the cyclopentadienyl rings are closer to the substituted carbon side.

Electrochemical Studies of *fac/mer*-$Mo(CO)_3$-(dppf)(η^2-C_{60}) (2), *mer*-$W(CO)_3$(dppf)(η^2-C_{60}) (3), and *mer*-$W(CO)_3$(dppf)(η^2-C_{70}) (5). Electrochemical studies on fullerenes exohedrally functionalized with ferrocene structural units are scanty,[18−20] although the coupling between the electron-donating ferrocene moieties and the electron-withdrawing fullerenes could potentially trigger interesting electronic properties in the field of high conductive materials or materials able to exhibit nonlinear optical properties.

Figure 5 compares the cyclic voltammetric cathodic response exhibited by the molybdenum complex **2** with that of the tungsten analogue **3** in 1,2-dichlorobenzene solution.

Apart from the original presence of minor traces of free C_{60} (hereafter, starred peaks underline the free fullerene reductions originating either from impurities or from byproducts of redox processes), **3** displays three main fullerene-centered reductions with features of chemical reversibility, which are shifted toward more negative potential values by about 0.2 V with respect to the corresponding processes of free C_{60}. By contrast, **2** proves to be notably unstable toward electron additions in that the second one-electron reduction just triggers C_{60} decomplexation. As a matter of fact, the most cathodic reduction now clearly involves the reduction of the fulleride dianion released as a consequence of the second cathodic step of the metallofullerene.

Figure 6 shows that the same fullerene-releasing effect occurs as a consequence of the metal-centered oxidations also in the case of the stable-to-reduction **3**. As a matter of fact, it is well evident that in the backscan the reductions of the free fullerene prevail over those of the metallocomplex.

In this connection, on the basis of previous results on the strictly related complexes containing redox-inactive diphosphines $Mo(CO)_3$(dppe)(η^2-C_{60}) and $W(CO)_3$(dppb) (η^2-C_{60}),[21] we are keen to attribute the first irreversible oxidation at about 1 V to the two-electron oxidation of the Mo(0) or W(0) center. More intriguing appears the localization of the expected one-electron oxidation of the coordinated dppf ligand. Under the present experimental conditions, free dppf undergoes a one-electron oxidation (coupled to chemical complications) at $E^{o\prime} = +0.89$ V. Because of the ill-defined profiles obtained in the anodic region for all the complexes, we do not venture

(18) Maggini, M.; Karlsson, A.; Scorrano, G.; Sandonà, G.; Farnia, G.; Prato, M. *J. Chem. Soc., Chem. Commun.* **1994**, 589.
(19) Bildstein, B.; Schweiger, M.; Angleitner, H.; Kopacka, H.; Wurst, K.; Ongania, K.-H.; Fontani, M.; Zanello, P. *Organometallics* **1999**, *18*, 4286.
(20) Bashilov, V. V.; Magdesieva, T. V.; Kravchuk, D. N.; Petrovskii, P. V.; Ginzburg, A. G.; Butin, K. P.; Sokolov,V. I. *J. Organomet. Chem.* **2000**, *599*, 37.
(21) Zanello, P.; Laschi, F.; Fontani, M.; Song, L.-C.; Zhu, Y.-H. *J. Organomet. Chem.* **2000**, *593−594*, 7.

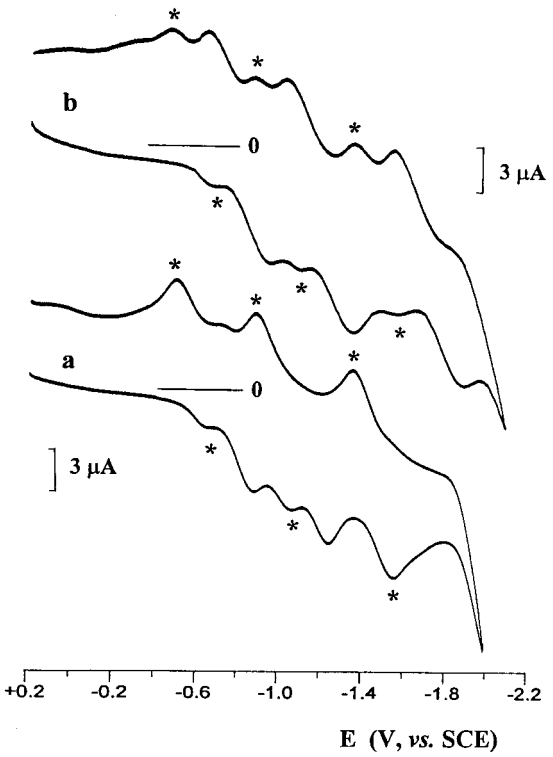

Figure 5. Cyclic voltrammetric responses recorded at a platinum electrode on 1,2-$C_6H_4Cl_2$ solutions containing $[NBu_4][PF_6]$ (0.08 mol dm^{-3}) and (a) **2** (0.4×10^{-3} mol dm^{-3}); (b) **3** (0.3×10^{-3} mol dm^{-3}). $T = 0$ °C. Scan rate 0.2 V s^{-1}.

to identify the oxidation at about 1.2 V as due to such a process, also in view of the fact that it follows a framework-destroying process.

The electrode potentials of the above-mentioned redox changes are compiled in Table 4, together with those of the C_{70} complex **5**, which will be discussed below.

It must be preliminarily pointed out that with respect to the theroretical peak-to-peak separation of 60 mV expected for electrochemically reversible one-electron processes, the large departures here observed must be attributed to the high solution resistivity caused by the low solubility of tetrabutylammonium supporting electrolyte in dichlorobenzene solvent. As a matter of fact, both C_{60} and C_{70}, which are known to undergo electrochemically reversible one-electron reductions, also display large peak-to-peak separations.

The negative shift of the fullerene-centered reductions caused by appended metal fragments with respect to free fullerene is a rather common feature in metallofullerene electrochemistry;[22] the effect is substantially due to the prevalence of the partial breaking of the double-bond conjugation operated by the η^2-coordination (which makes the reduction more difficult) over the inductive effects of the exohedral metallic fragment (which can favor or disfavor the reduction). Rather unexpectedly, in the present case, in which a ferrocene donor ligand is present in the appended diphosphine, the negative shift of about 0.2 V is substantially similar to that previously recorded for the related complexes

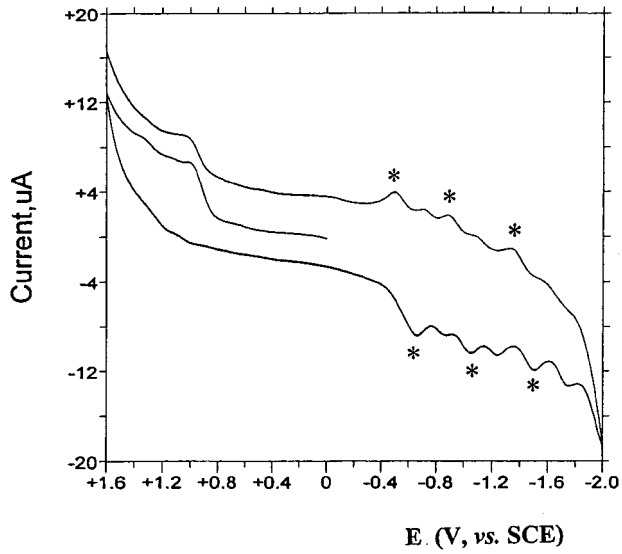

Figure 6. Cyclic voltammetric response recorded at a platinum electrode on a 1,2-$C_6H_4Cl_2$ solution containing $[NBu_4][PF_6]$ (0.08 mol dm^{-3}) and **3** (0.3×10^{-3} mol dm^{-3}). $T = 0$ °C. Scan rate 0.2 V s^{-1}.

(η^2-C_{60})$Mo(CO)_3$(dppe) and (η^2-C_{60})$W(CO)_3$(dppb).[21] This seems to indicate that no significant electronic interaction takes place between the ferrocendiyldiphosphine and the fullerene unit. As above-discussed, unfortunately we cannot further support such a conclusion making use of the eventual anodic shift of dppf oxidation.

Figure 7 shows the cyclic voltammetric response of **5** in comparison with that of free C_{70}.

At variance with **3**, which proved to be stable toward multiple one-electron reductions, **5** adds reversibly the first two electrons, whereas the third reduction induces releasing of C_{70}^{3-}. This account for the fact that the fourth reduction looks like a two-electron reduction: the fourth one-electron reduction of the metallofullerene couples with that of the released C_{70}^{3-} (ECE mechanism).

It is useful to note from Table 4 that the negative shift in reduction potentials induced by the $W(CO)_3$(dppf) fragment with respect to free C_{70} is about 0.1 V, i.e., significantly lower than that induced by the same fragment with respect to C_{60}. Such an effect has been previously observed for the couple $Mo(CO)_2$(phen)(dbm)-(η^2-C_{60})/$Mo(CO)_2$(phen)(dbm)(η^2-C_{70}),[23] thus supporting that the double-bond saturation operated by η^2-metal coordination to C_{70} is lower than that relative to C_{60}.

Experimental Section

General Comments. All reactions were carried out under an atmosphere of highly purified nitrogen using standard Schlenk or vacuum-line techniques. Acetonitrile and chlorobenzene were dried by distillation from P_2O_5 and CaH_2 under nitrogen. Pentane and THF were distilled under nitrogen from sodium/benzophenone ketyl. [60]Fullerene (99.9%) and [70]-fullerene (98%) were of commercial origin. $Mo(CO)_3(CH_3CN)_3$,[24] 1,1′-bis(diphenylphosphino)ferrocene (dppf),[25] $Mo(CO)_4$(dppf),[26] and $W(CO)_4$(dppf)[26] were prepared according to literature

(22) Zanello, P. Electrochemical and Structural Aspects of Metallofullerenes. In *Chemistry at the Beginning of the Third Millennium*; Fabbrizzi, L., Poggi, A., Eds., Springer-Verlag: Heidelberg, 2000; p 247.

(23) Zanello, P.; Laschi, F.; Cinquantini, A.; Fontani, M.; Tang, K.; Jin, X.; Li, L.*Eur. J. Inorg. Chem.* **2000**, 1345.

(24) Tate, D. P.; Knipple, W. R.; Augl, J. M. *Inorg. Chem.* **1962**, *1*, 433.

Table 4. Formal Electrode Potentials (in V, vs SCE) and Peak-to-Peak Separation (in mV) for the Redox Changes Exhibited by the Metallofullerenes $M(CO)_3(dppf)$ (η^2-C_x) (x = 60, 70; M = Mo, W) and Related Species in 1,2-$C_6H_4Cl_2$ Solution

		fullerene-centered reductions							Mo(W)-centered oxidation	
M [C_x]	T (°C)	$E^{o\prime}_{0/-}$	ΔE_p[a]	$E^{o\prime}_{-/2-}$	ΔE_p[a]	$E^{o\prime}_{2-/3-}$	ΔE_p[a]	$E^{o\prime}_{3-/4-}$	ΔE_p[a]	E_p
W [C_{60}]	20	−0.78	150	−1.17	140	−1.74[a,b]				+1.00
	0	−0.81	220	−1.19	230	−1.70	250			*c*
Mo[C_{60}]	20	−0.79	140	−1.21[a,b]						+0.95
	0	−0.79	170	−1.16	180	−1.74[a,b]				*c*
C_{60}	20	−0.60	210	−1.00	230	−1.45	270			
	0	−0.63	208	−1.04	240	−1.48	280			
W [C_{70}]	20	−0.73	180	−1.04	200	−1.54[a,b]				+0.97
	0	−0.74	162	−1.11	154	−1.47	182			*c*
C_{70}	20	−0.53	186	−0.92	202	−1.33	192	−1.75	174	
	0	−0.57	260	−0.96	276	−1.39	300			

[a] Measured at 0.2 Vs^{-1}. [b] Peak potentials for irreversible processes. [c] Not measured.

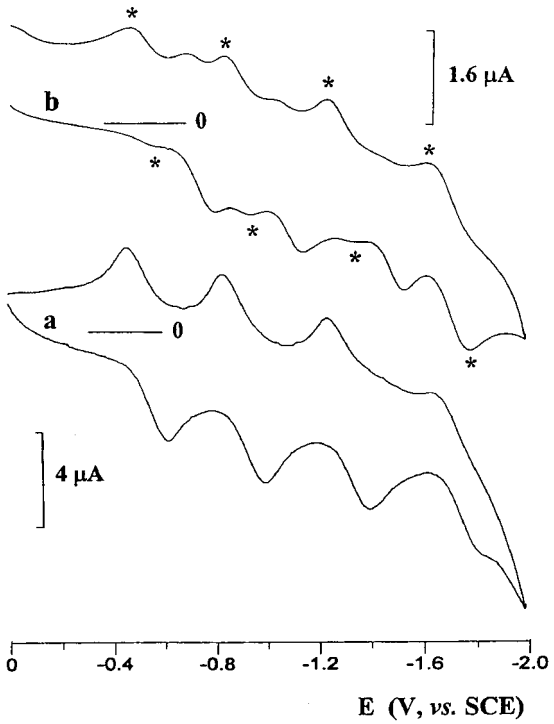

Figure 7. Cyclic voltammetric responses recorded at a platinum electrode on 1,2-$C_6H_4Cl_2$ solutions containing [NBu_4][PF_6] (0.08 mol dm^{-3}) and (a) C_{70} (0.5×10^{-3} mol dm^{-3}); (b) **5** (0.2×10^{-3} mol dm^{-3})). T = 20 °C.

procedures. Products were separated by thin-layer chromatography (TLC glass plates of 20 × 25 × 0.25 cm coated with silica gel 60H) or by column chromatography (30 × 2.5 cm column with silica gel). Melting points were determined on a Yanaco MP-500 apparatus. Elemental analysis and FAB-MS were performed on a Yanaco CHN Corder MT-3 analyzer and a Zabspec spectrometer. IR and UV−vis spectra were recorded on a Bio-Rad FTS 135 and a Shimadzu UV-2401/PC spectrometers. ^{1}H NMR, ^{31}P NMR, and ^{13}C NMR spectra were obtained on a Bruker AC-P200 or a UNITY Plus-400 spectrometer.

Synthesis of *fac*-$Mo(CO)_3(dppf)(CH_3CN)$ (1). A 100 mL two-necked flask equipped with a stir-bar, a serum cap, and a reflux condenser topped with a N_2 inlet tube was charged with 0.15 g (0.50 mmol) of $Mo(CO)_3(CH_3CN)_3$, 0.277 g (0.50 mmol) of dppf, and 35 mL of acetonitrile. The mixture was stirred and refluxed for 30 h. The warm solution was filtered and refrigerated overnight. A crop of 0.198 g (51%) of **1** was isolated as golden crystals. Mp: 210−212 °C dec. Anal. Calcd for $C_{39}H_{31}FeMoNO_3P_2$: C, 60.41; H, 4.03; N, 1.81. Found: C, 60.49; H, 4.23; N, 1.86. IR (KBr disk): $\nu_{C\equiv O}$, 1926(vs), 1826(vs), 1808(vs) cm^{-1}. ^{1}H NMR (200 MHz, $CDCl_3$, TMS): 1.98(s, 3H, CH_3), 4.24(s, 4H, C_5H_4), 4.29(s, 4H, C_5H_4), 7.20−7.60(m, 20H, $4C_6H_5$,) ppm. ^{31}P NMR (81 MHz, $CDCl_3$, H_3PO_4): 37.86(s) ppm.

Synthesis of *fac/mer*-$Mo(CO)_3(dppf)(\eta^2$-$C_{60})$ (2). Method (i). A 100 mL two-necked flask equipped with a stir-bar, a N_2 inlet tube, and a serum cap was charged with 0.036 g (0.050 mmol) of C_{60} and 50 mL of chlorobenzene. The mixture was stirred at room temperature until all C_{60} was dissolved. To the solution was added 0.039 g (0.050 mmol) of complex **1**, and the reaction mixture was heated to about 90 °C and stirred at this temperature for 2 h, during which time the purple solution turned dark green. The resulting solution was evaporated at reduced pressure, and the residue was separated by column chromatography using 1:1 (v/v) toluene−light petroleum ether as eluent under an atmosphere of highly purified nitrogen. From the first purple band unreacted C_{60} was recovered, and from the chlorophyll-green band 0.015 g (21%) of **2** as a dark green solid was obtained.

Method (ii). A 100 mL photoreactor equipped with a N_2 inlet tube and a serum cap was charged with 0.072 g (0.10 mmol) of C_{60}, 0.078 g (0.10 mmol) of $Mo(CO)_4$(dppf), and 50 mL of chlorobenzene. The photoreactor containing the resulting purple solution was evacuated to a pressure of ca. 0.1 mmHg, and then the solution was irradiated by a water-cooled UV 450 W mercury vapor lamp for 2 h, with periodic evacuation of CO to give a dark green solution. Through the same workup used in method (i) 0.126 g (87%) of **2** was obtained. Recrystallization from toluene and pentane gave complex **2** as dark green crystals. Mp: 300 °C dec. Anal. Calcd for $C_{97}H_{28}FeMoO_3P_2$: C, 80.07; H, 1.97. Found: C, 79.98; H, 2.05. IR (KBr disk): $\nu_{C\equiv O}$, 2000(s), 1972(w), 1936(s), 1920(s), 1882(vs); ν_{C60}, 1434(m), 1185(w), 585(w), 526(s) cm^{-1}. UV−vis (THF, 9.21×10^{-6} M) λ_{max}(log ϵ): 239.0 (4.94), 256.7 (5.25), 329.3 (4.74), 436.3 (3.89), and 598.7 (3.55) nm. ^{1}H NMR (200 MHz, CS_2, TMS): 4.13 (s, 4 H, C_5H_4), 4.49, 4.65 (2s, 4 H, C_5H_4), 7.18−7.69 (m, 20 H, $4C_6H_5$) ppm. ^{31}P NMR (81 MHz, $C_6D_4Cl_2$, H_3PO_4): 39.31(d, 1P, J_{P-P} = 33.2 Hz), 33.56(s, 2P), 29.86(d, 1P, J_{P-P} = 33.2 Hz) ppm.

Synthesis of *mer*-$W(CO)_3(dppf)(\eta^2$-$C_{60})$ (3) and $[W(CO)_3(dppf)]_2(\eta^2,\eta^2$-$C_{60})$ (4). The same synthetic procedure, namely, method (ii), for preparation of **2** was employed, except that 0.086 g (0.10 mmol) of tungsten complex $W(CO)_4$(dppf) was used instead of molybdenum complex $Mo(CO)_4$(dppf) and the reaction mixture was separated by TLC using 1:1 (v/v) toluene−light petroleum ether as eluent under anaerobic conditions. The first band gave a small amount of C_{60}. From the chlorophyll-green band 0.135 g (87%) of **3** was obtained, which was further recrystallized from THF and pentane to give **3** as dark green crystals. Mp: 300 °C dec. Anal. Calcd for $C_{97}H_{28}FeO_3P_2W$: C, 75.51; H, 1.83. Found: C, 75.53; H, 2.04. IR (KBr disk): $\nu_{C\equiv O}$, 1998(s), 1936(s), 1868(vs); ν_{C60}: 1434(m),

(25) Bishop, J. J.; Davison, A.; Katcher, M. L.; Lichtenberg, D. W.; Merrill, R. E.; Smart, J. C. *J. Organomet. Chem.* **1971**, *27*, 241.
(26) Rudie, A. W.; Lichtenberg, D. W.; Katcher, M. L.; Davison, A. *Inorg. Chem.* **1978**, *17*, 2859.

Table 5. Crystal Data and Structure Refinements for *fac*-Mo(CO)$_3$(dppf)(CH$_3$CN)·0.5H$_2$O, W(co)$_4$(dppf), and *mer*-W(CO)$_3$(dppf)(η^2-C$_{60}$)·C$_6$H$_5$CH$_3$

	fac-Mo(CO)$_3$(dppf)(CH$_3$CN)·0.5H$_2$O	W(CO)$_4$(dppf)	*mer*-W(CO)$_3$(dppf)(η^2-C$_{60}$)·C$_6$H$_5$CH$_3$
mol formula	$C_{39}H_{32}FeMoNO_{3.5}P_2$	$C_{38}H_{28}FeO_4P_2W$	$C_{104}H_{36}FeO_3P_2W$
mol wt	784.39	850.24	1634.97
temp/K	298	298	298
cryst syst	$P2_1/n$	$P\bar{1}$	$P\bar{1}$
space group	monoclinic	triclinic	triclinic
a/Å	12.0503(8)	10.2520(10)	13.7178(7)
b/Å	21.5612(16)	10.9481(10)	15.4457(8)
c/Å	13.7949(10)	18.0955(17)	17.5888(10)
α/deg		82.602(2)	72.1920(10)
β/deg	96.911(2)	76.713(2)	75.3730(10)
γ/deg		85.280(2)	64.7640(10)
V/Å^3	3558.1(4)	1957.3(3)	3177.1(3)
Z	4	2	2
D_c/g·cm^{-3}	1.464	1.443	1.709
abs coeff/mm^{-1}	0.889	3.423	2.155
F(000)	1596	836	1628
θ range for data collecn/deg	1.76 to 25.03	1.88 to 25.03	1.23 to 25.03
no. of rflns	14 691	8154	13 177
no. of indep rflns	6295	6836	11 142
R_{int}	0.0218	0.0252	0.0254
completeness to $\theta = 25.03°$	99.9%	99.3%	99.3%
no. of data/restraints/params	6295/3/445	6836/0/415	11 142/0/988
goodness of fit on F^2	1.053	1.027	1.008
final R indices [$I>2\sigma(I)$]	R1 = 0.0254, wR2 = 0.0592	R1 = 0.0402, wR2 = 0.0994	R1 = 0.0370, wR2 = 0.0812
R indices (all data)	R1 = 0.0332, wR2 = 0.0625	R1 = 0.0551, wR2 = 0.1055	R1 = 0.0536, wR2 = 0.0884
largest diff peak and hole/e Å^{-3}	0.334 and −0.267	1.306 and −1.215	0.632 and −0.944

1186(w), 585(w), 526(s) cm^{-1}. UV−vis (THF, 8.30 × 10^{-6} M) λ_{max}(log ϵ): 238.2(5.05), 257.1(5.14), 333.5(4.58), 433.0 (4.08), 598.3(3.64) nm. ^{1}H NMR (200 MHz, CS_2, TMS): 4.15(s, 4 H, C_5H_4), 4.52, 4.70 (2s, 4 H, C_5H_4), 7.20−7.70(m, 20H, 4C_6H_5) ppm. ^{31}P NMR (81 MHz, $C_6D_4Cl_2$, H_3PO_4): 18.47(d, J_{P-P} = 30.8 Hz, 1P), 12.79(d, J_{P-P} = 30.8 Hz, 1P) ppm. FAB MS: m/z 1542 (W(CO)$_3$(dppf)(η^2-C$_{60}$)$^+$, ^{56}Fe, ^{184}W). ^{13}C NMR (100.6 MHz, $CDCl_3$, TMS, 25 °C): 206.00 (1C, CO), 204.57(1C, CO), 203.95-(1C, CO), 163.70(4C), 147.46(4C), 146.61(2C), 145.55(4C), 145.29(2C), 145.18(4C), 144.64(8C), 143.94(4C), 143.36(4C), 142.90(2C), 142.67(4C), 142.17(4C), 142.03(4C), 140.20(4C), 137.99(2C), 137.77(2C), 79.34(2C)(C$_{60}$ resonances), 135.30(d, $^2J_{P-C}$ = 10.8 Hz), 134.59(d, $^2J_{P-C}$ = 10.8 Hz), 133.45(d, J = 6.1 Hz), 133.40(d, J = 5.4 Hz), 131.08(d, J = 30.78 Hz), 130.00-(s), 128.58(s), 128.25(s) (P(C_6H_5)$_2$ resonances); 77.48, 76.19, 75.33, 74.59, 72.45, 71.34 (C_5H_4 resonances) ppm. The third band gave 0.015 g (13% based on W(CO)$_4$(dppf)) of **4**, which was recrystallized from THF and pentane to afford **4** as a black solid. Mp: 300 °C dec. Anal. Calcd for $C_{134}H_{56}Fe_2O_6P_4W_2$: C, 68.05; H, 2.39. Found: C, 67.78; H, 2.61. IR (KBr disk): $\nu_{C\equiv O}$, 1995(s), 1929(s), 1870(vs); ν_{C60}: 1434(m), 804(s), 605(m), 514-(m) cm^{-1}. UV−vis (THF, 8.46 × 10^{-6} M) λ_{max} (log ϵ): 239.3-(5.18), 255.5(5.20), 333.5(sh, 4.67), 430.5(4.21), 599.0(3.65) nm. ^{1}H NMR (200 MHz, CS_2, TMS): 4.02−4.28(m, 4 H, C_5H_4), 4.40−4.80(m, 4 H, C_5H_4), 7.10−7.80(m, 20H, 4C_6H_5) ppm. ^{31}P NMR (81 MHz, CS_2, H_3PO_4): 23.67(s, 2P), 16.94(s, 2P) ppm.

Synthesis of *mer*-W(CO)$_3$(dppf)(η^2-C$_{70}$) (5) and [*mer*-W(CO)$_3$(dppf)]$_2$(η^2,η^2-C$_{70}$) (6). The same synthetic procedure, namely, method (ii), for preparation of **2** was utilized, except that 0.043 g (0.10 mmol) of tungsten complex W(CO)$_4$(dppf) and 0.042 g (0.05 mmol) of C$_{70}$ were used in place of molybdenum complex Mo(CO)$_4$(dppf) and C$_{60}$. The reaction mixture was separated by TLC using 1:1 (v/v) toluene−light petroleum ether as eluent under anaerobic conditions. The first band gave a small amount of C$_{70}$. From the second band was obtained 0.042 g (51%) of **5**, which was recrystallized from THF and pentane to afford **5** as a black solid. Mp: 300 °C dec. Anal. Calcd for $C_{107}H_{28}FeO_3P_2W$: C, 77.28; H, 1.70. Found: C, 77.07; H, 1.95. IR (KBr disk): $\nu_{C\equiv O}$, 1999(s), 1937(s), 1870(vs); ν_{C70}: 1636(m), 1433(s), 1123(w), 1037(w), 795(w), 673(s), 672(m), 535(m) cm^{-1}. UV−vis (THF, 4.93 × 10^{-6} M) λ_{max} (log ϵ): 239.5(5.39), 330.0(sh, 4.74), 350.0(4.69), 377.5(4.65), 426.9(4.60), 457.1(4.63), 598.3(4.12) nm. ^{1}H NMR (200 MHz, CS_2, TMS): 4.12(s, 4 H, C_5H_4), 4.50, 4.62(2s, 4 H, C_5H_4), 7.10−7.85(m, 20H, 4C_6H_5) ppm. ^{31}P NMR (161.95 MHz, $CDCl_3$, H_3PO_4): 16.65-(br, 2P), 10.20(br, 2P) ppm. FAB-MS, m/z: 1663 [W(CO)$_3$(dppf)(η^2-C$_{70}$)H$^+$,^{184}W, ^{56}Fe]. The third red-brown band gave 0.030 g (48%) of **6** as a red-brown solid. Mp: 300 °C dec. Anal. Calcd for $C_{144}H_{56}Fe_2O_6P_4W_2$: C, 69.59; H, 2.27. Found: C, 69.52; H, 2.37. IR (KBr disk): $\nu_{C\equiv O}$, 1998(s), 1935(s), 1870(vs); ν_{C70}, 1630-(m), 1433(s), 1037(m), 795(w), 673(w), 536(m) cm^{-1}. UV−vis (THF, 4.43 × 10^{-6} M) λ_{max} (log ϵ): 238.1 (5.14), 330.0(4.51), 362.5(4.45), 378.0(4.43), 456.7(4.42) nm. ^{1}H NMR(200 MHz, CS_2, TMS): 4.10(br, 4 H, C_5H_4), 4.47, 4.63 (2s, 4 H, C_5H_4), 7.20−7.70(m, 20H, 4C_6H_5) ppm. ^{31}P NMR(161.95 MHz, C_6D_6, H_3PO_4): centered at 12.27(m, 2P), centered at 5.54(m, 2P) ppm.

X-ray Crystallography. Single crystals of **1** suitable for X-ray diffraction analysis were obtained by evaporation of its acetonitrile solution at about 5 °C, whereas single crystals of W(CO)$_4$(dppf) and **3** were obtained by evaporation of their toluene solutions at room temperature. The single crystal of **1** (0.30 × 0.25 × 0.15 mm), that of W(CO)$_4$(dppf) (0.20 × 0.25 × 0.30 mm), and that of **3** (0.20 × 0.25 × 0.30 mm) were glued to a glass fiber and mounted on a Bruker SMART 1000 automated diffractometer. Data were collected at room temperature, using Mo Kα graphite monochromator radiation (λ = 0.71073 Å) in the ω scanning mode. Absorption corrections were performed using SADABS for all of them. The structures were solved by direct methods using the SHELXTL-97 program and refined by full-matrix least-squares techniques (SHELXL-97) on F^2. Hydrogen atoms were located by using the geometric method. The weighting scheme $w = 1/\sigma^2(F_o^2) + (0.0777P)^2$ (where $P = (F_o^2 + 2F_c^2)/3$) was applied to the data for **1**, $w = 1/\sigma^2(F_o^2) + (0.0578P)^2$ (where $P = (F_o^2 + 2F_c^2)/3$) was applied to the data for W(CO)$_4$(dppf), and $w = 1/\sigma^2(F_o^2) + (0.0422P)^2$ (where $P = (F_o^2 + 2F_c^2)/3$) was applied to the data for **3.** The crystal data and structural refinements details are listed in Table 5.

Electrochemistry. Materials and apparatus for electrochemistry have been described elsewhere.[27] 1,2-Dichlorobenzene, anhydrous, 99% (Aldrich), was used as solvent; electrochemical grade [NBu$_4$][PF$_6$] (Fluka) was used as supporting electrolyte (0.08 mol dm^{-3}). All the potential values are

(27) Zanello, P.; Laschi, F.; Fontani, M.; Mealli, C.; Ienco, A.; Tang, K.; Jin, X.; Li, L. *J. Chem. Soc., Dalton Trans.* **1999**, 965.

referred to the saturated calomel electrode (SCE). Under the present experimental conditions, the one-electron oxidation of ferrocene occurs at $E^{\circ\prime} = +0.55$ V at +20 °C and $E^{\circ\prime} = +0.56$ V at 0 °C.

Acknowledgment. We are grateful to the National Natural Science Foundation of China, the Research Fund for the Doctoral Program of Higher Education of China, and the Laboratory of Organometallic Chemistry for financial support. Piero Zanello gratefully acknowledges the financial support of the University of Siena.

Supporting Information Available: Full tables of crystal data, atomic coordinates and thermal parameters and bond lengths and angles for **1**, $W(CO)_4$(dppf), and **3**. This material is available free of charge via the Internet at http://pubs.acs.org.

OM000579+